Anisotropic 1H STD-NMR Spectroscopy: Exploration of Enantiomer-Polypeptide Interactions in Chiral Oriented Environments

Boris Gouilleux, Francois-Marie Moussallieh, Philippe Lesot

Anisotropic ^{1}H STD-NMR Spectroscopy: Exploration of Enantiomer-Polypeptide Interactions in Chiral Oriented Environments

Boris Gouilleux,[a] Francois-Marie Moussallieh,[a] and Philippe Lesot*[a,b]

[a] Université Paris-Saclay, UFR d'Orsay, RMN en Milieu Orienté, ICMMO, UMR CNRS 8182, Bât. 410, 15, rue du Doyen Georges Poitou, F-91405 Orsay cedex, France.

[b] Centre National de la Recherche Scientifique (CNRS), 3, rue Michel Ange, F-75016 Paris, France.

In memory of Prof. Aharon Loewenstein (1929-2022).

Abstract:

We explore and report for the first time the use of ^{1}H saturation transfer difference NMR experiments (STD-NMR) in weakly-aligning chiral anisotropic media to identify the hydrogen sites of enantiomers of small chiral molecules interacting with the side-chain of poly-γ-benzyl-L-glutamate (PBLG), a helically chiral polypeptide polymer. The first experimental results obtained on three model mono-stereogenic compounds outcomes are highly promising and demonstrate the possibility to track down possible differences of spatial position of enantiomers at the vicinity of the polymer side-chain. Anisotropic STD experiments appear to be well suited for rapid screening of chiral analytes that bind favorably to orienting polymeric systems, while providing new insights into the mechanism of enantio-discrimination without resorting to the time-consuming determination of molecular order parameters.

Keywords: ^{1}H STD-NMR, PBLG-based Liquid Crystals, Enantiodiscrimination, Molecular interactions, Epitope mapping.

Supporting information: Electronic information available for this article

Corresponding author: philippe.lesot@universite-paris-saclay.fr

Authors: Dr. Boris Gouilleux, Dr. Francois-Marie Moussallieh and Dr. Philippe Lesot (DR CNRS)

ORCID Id: **BG :** 0000-0002-6491-3525
FMM : 0000-0003-2508-6472
PL*: 0000-0002-5811-7530

Introduction

NMR spectroscopy in polymer-based, lyotropic chiral liquid crystals (CLC) is a powerful analytical tool to address many issues of molecular enantiodiscrimination, enantiopurity determination and stereochemistry.[1,2,3] These aligned media, which are formed by organic solutions of helically chiral homopolymers oriented with their main axes parallel to the static magnetic field $\mathbf{B_0}$, interact differently with enantiomers of a guest chiral molecule, so that they exhibit a different orientation, on average, relative to $\mathbf{B_0}$. Investigating and evaluating the interaction processes is therefore a key step to understand the whole enantiodiscrimination mechanisms in these orienting systems.[4,5]

The molecular orientation may be represented by a Saupe matrix, $\langle S_{\alpha\beta}\rangle^{R,S}$, or an alignment tensor, $\langle A_{\alpha\beta}\rangle^{R,S} = \frac{2}{3}\langle S_{\alpha\beta}\rangle^{R,S}$, which are different for both enantiomers when the enantiodiscrimination occurs as demonstrated from 1995.[4] The bracket symbol corresponds to an ensemble average. This orientation difference leads to a spectral discrimination of enantiomers based on variations of residual anisotropic observables, Obs^{aniso}, namely dipolar coupling (RDC), chemical shift anisotropy (RCSA) or quadrupolar coupling (RQC).[6] All can be simply expressed as the product of constant value - depending on the nature of the interaction - and the Saupe tensor elements (**Eq. 1**).[1]

$$\langle Obs^{aniso}\rangle^{R \text{ or } S} = K\langle S_{\alpha\beta}\rangle^{R \text{ or } S} \qquad (\mathbf{1})$$

These NMR interactions have been successfully exploited in structural/conformational studies, in the determination of 3D structures, relative configurations[7,8,9,10] or in the measurement of enantiomeric excesses, …[1,2] However, the underlying principles governing the enantio-discrimination mechanisms, *i.e.* the difference between $\langle S_{\alpha\beta}\rangle^{R}$ and $\langle S_{\alpha\beta}\rangle^{S}$, are still under investigation.[11,12,13]

This understanding is of major importance for: i) determining the absolute configuration of stereogenic centers from NMR residual anisotropic data (RDC, RCSA, RQC) supported by computational simulations (molecular dynamics),[14,15,16,17,18] ii) designing the structure of new efficient polymeric-based lyotropic liquid crystal, *e.g.* choice of the polymer,[19,20,21,22] or iii) optimizing the choice of co-solvent (polarity), the sample component concentration, the presence or not of additives,[23] to enhance the enantio-discrimination abilities.

Previous studies have assessed and compared the enantio-discrimination either for a given chiral solute in regards to various polymeric-based CLC, or rather for a collection of analytes dissolved in similar mesophases. This can be evaluated by measuring the local differential

ordering effect (DOE) using selectively deuterated analytes[24] or at a more global level by comparing $\langle S_{\alpha\beta}\rangle^{R,S}$ for both enantiomers (variation of principal axis direction, 9D angle, …) determined using anisotropic data such as (^{1}H-^{1}H)-RDC, (^{13}C-^{1}H)-RDC and more recently ^{2}H-RQC.[1,2,6,11] While more comprehensive and reliable, this approach is sometimes time-consuming and requires a sufficient amount of anisotropic data to determine the Saupe's matrices, $\langle S_{\alpha\beta}\rangle^{R,S}$, (over 5 for C_1-symmetry chiral molecules).[25]

Moreover, it is worth noting the average nature of these calculated tensors, which encompasses the orientational behavior of the chiral analyte both at the vicinity of the polymer ("bound" analyte) and in the bulk of the mesophase ("free" analyte). In a fast exchange dynamic regime, this situation may be represented by a simple two-site model, as expressed by **Eq. 2**:[26]

$$\langle S_{\alpha\beta}\rangle_{obser}^{R\ or\ S} = f_b\langle S_{\alpha\beta}\rangle_b^{R \text{ or } S} + (1-f_b)\langle S_{\alpha\beta}\rangle_f^{R \text{ or } S}. \qquad (\mathbf{2})$$

In this equation, f_b is the fraction of "bound" analytes, $\langle S_{\alpha\beta}\rangle_b^{R,S}$ and $\langle S_{\alpha\beta}\rangle_f^{R,S}$ are the Saupe matrix corresponding to the "bound" and "free" analytes, respectively. In this modeled view, we may safely assume that the term $(1-f_b)$ is close to 1, while the elements in order matrix $\langle S_{\alpha\beta}\rangle_f^{R,S}$ are close to zero, namely the order of the analytes is negligible when they are mainly surrounded by the organic solvent (bulk).

From **Eq. 2**, the enantio-discrimination phenomenon leading to $\langle S_{\alpha\beta}\rangle^R \neq \langle S_{\alpha\beta}\rangle^S$ mainly arises from: i) enantioselective diastereomorphous interactions between enantiomers and the chiral polymer side-chains, *i.e.* $\langle S_{\alpha\beta}\rangle_b^R \neq \langle S_{\alpha\beta}\rangle_b^S$, and ii) from affinity differences between *R* or *S* isomers and the chiral polymer involving a difference of bound fraction, *i.e.* $f_b^R \neq f_b^S$, or iii) both of them. Therefore, the direct investigation of the chiral analyte-polymer interactions is of major interest to further understand the enantio-discrimination mechanisms.[26]

To this aim, we propose to characterize directly the oriented transient polymer-analyte array by saturation transfer difference (STD) NMR spectroscopy.[27,28] This is a well-established method to probe and characterize small molecules in weak interaction with a macromolecule based on intermolecular magnetization transfers. It has been widely used to assess ligand-protein interactions both in terms of affinity (determination of dissociation constants K_D) and geometry (epitope mapping).[27,28,29,30,31]

Interestingly, this tool has also been employed for investigating polar solutes interacting with soft matters (as stationary phases used in HPLC) by ^{1}H high-resolution magic angle spinning (HR-

at low speed) techniques,[32] as well as applied successfully to characterize enantiomers-macromolecule interactions in achiral isotropic liquids.[33,34,35,36] However, STD-NMR approach has never been tested so far to investigate the case of chiral lyotropic liquid crystals, to the best of our knowledge.

In this exploratory work, we report the first ^{1}H STD-NMR experiments performed in a polypeptide CLC (PBLG), a well-known and effective enantiodiscriminating polymer, in presence of various chiral secondary alcohols (R_4-C*H(OH)(CH_3)): hexan-2-ol (**HL**), 1-phenethyl alcohol (**PL**) and 3-butyn-2-ol (**BL**) (see **Figure 2** and **SI-1**). These analytes are interesting chiral model compounds with common features: a marked shape anisotropy around the stereogenic center as well as an active site promoting H-bonding, but with different types of substituent that may either allow π-π or van-der-Waals interactions. Under these conditions, we anticipate that a STD-NMR approach may deliver valuable insights on difference of enantio-orientations at the vicinity of the polymer side-chains (difference in $\langle S_{\alpha\beta}\rangle_b^{R,S}$) and/or affinity ($f_b$).

After describing the method, this article reports: i) a qualitative ^{1}H STD-NMR study to screen model chiral secondary alcohols that bind to the PBLG polymer as well as the identification of solute interacting sites; ii) a quantitative STD-NMR analysis carried out with an acetylenic chiral alcohol to highlight and characterize differential epitope mapping of the two enantiomers with respect to PBLG. This analysis is performed both on enantiopure samples and on a racemic mixture.

Results and Discussion

Anisotropic ^{1}H STD-NMR to screen chiral analytes interacting with PBLG. The basic principle of ^{1}H STD-NMR in anisotropic media is formally identical to that applied to isotropic samples.[27,28,29,30,31] Hence, from a practical point of view, the anisotropic STD-NMR experiments can be performed using the routine STD-NMR pulse sequence developed in isotropic liquids, with no peculiar modification (see **Figure SI-2**).

In anisotropic ^{1}H STD-NMR experiments, an adequate spectral region of the oriented polypeptide (PBLG) is selectively irradiated (saturated) while leaving those of the enantiomers unaffected. During the saturation process, ^{1}H magnetization is mainly transferred throughout spin-diffusion to the polymer-side chain nuclei (most accessible region of the polymer due its high flexibility) under interaction with the oriented solutes. The intermolecular NOE between the polymer and enantiomer spins leads to a transfer of magnetization from the polymer to solute

molecules in a "bound" state, which is then shared with those in the bulk by a rapid exchange between the "bound" and "free" states. A scheme of this process is shown in **Figure 1a**. As this magnetization transfer impacts the signal intensity of the solute, substracting the ^{1}H spectra recorded in the absence ("off-experiment") and presence ("on-experiment") of polymer saturation leads to a differential spectrum, called the "anisotropic STD spectrum", which is non-zero or zero for interacting or non-interacting enantiomers, respectively. Amplification factors, STD_i, can be then determined as the intensity (or area) ratio between the remaining signals on the STD spectrum and on the reference spectrum (off-experiment) as:

$$STD_i^{R,S}\ (\%) = \left[\frac{I_{Off}^{R,S}(i) - I_{On}^{R,S}(i)}{I_{On}^{R,S}(i)}\right] \times 100 \qquad (3)$$

In **Eq. 3**, the terms, $I_{Off}^{R,S}(i)$ and $I_{On}^{R,S}(i)$, correspond to the signal intensity (or area) of a site i of the analyte measured with the “off-experiment” and “on-experiment”, respectively (see **Figure 1b**). The superscripts *R* and *S* highlight the fact that enantiomers potentially lead to different STD amplification factors for a given chiral molecule dissolved in an enantiodiscriminating mesophase.

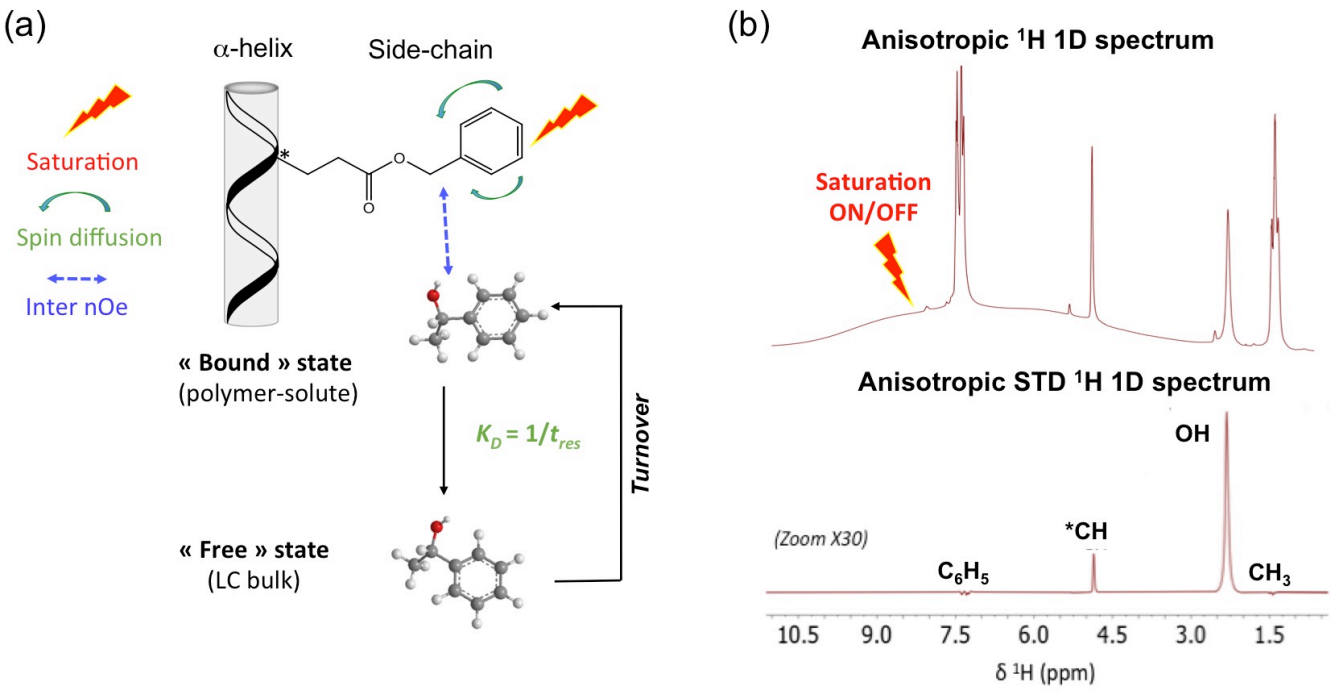

Figure 1. (a) Schematic principle of anisotropic STD-NMR using PBLG polymer as CLC and (*S*)-**PL** as solute. K_D and t_{res} correspond to the dissociation constant and the time-residence of the transient polymer-solute complex, respectively, while LC stands for liquid crystal. (b) One example of anisotropic ^{1}H NMR (top) and anisotropic ^{1}H STD-NMR spectrum (bottom) recorded in PBLG/CD_2Cl_2 (295 K) at 600 MHz. Here the (*S*)-**PL** is used as chiral solute. Note the very broad ^{1}H signal (centered around 7.3 ppm) corresponding to the aromatic ^{1}H sites of the PBLG side-chain in **1b** (top). A baseline correction is applied on the STD spectrum (bottom). Weak negative signals for phenyl and methyl groups are artefacts arising from imperfect on/off-spectra subtraction.

As they are based on an intermolecular NOE, the STD amplification factors are more important if the interacting nuclei are spatially closed, reflecting the spatial proximity of the chiral solute towards the polymer side-chains in the “bound” state. Thus, the distribution of the STD values (*i.e.* epitope mapping) for each enantiomer may deliver new and valuable insights on the mechanisms of enantiodiscriminations in PBLG phases. Besides the efficiency of intermolecular polymer-solute NOE, the magnitude of STD signals also depends on accumulation of molecules labeled by the magnetization transfer in the bulk during the saturation process. This is driven by the duration of polymer saturation, t_{sat}, as well as the exchange features between “bound” and “free” states.[28, 29,37] This latter corresponds to the time-residence, t_{res}, of the transient polymer-solute complex and fractions of solutes in both states as well (see **Figure 1a**).

Contrarily to STD-NMR in liquids, anisotropic STD-NMR experiments investigate solute molecules that are oriented on average in the magnetic field, and hence it could be argued that site-specific ^{1}H STD amplification factors measured in liquid crystals is biased by possible anisotropic dipolar relaxation mechanisms ('intermolecular NOE'). In the case of (weakly aligning) PBLG-based lyotropic systems, we may safely assume that this bias does not exist (at least significantly). Indeed whether the main relaxation processes of solute (dipolar mechanisms for ^{1}H and quadrupolar mechanisms for ^{2}H) are sensitive to solute molecular ordering, S, the spectral density $J(\omega)$ shows a dependence in S^2 in a first approximation.[38] Thus, when the solute ordering is small ($S < 10^{-3}$), the S^2 dependency on « anisotropic » ^{1}H dipolar relaxation mechanism is negligible, and so the classical isotropic relaxation models (used to explain the ^{1}H STD-NMR) remain valid.[39] In the PBLG mesophases, solute ordering is ranging between 10^{-3} and 10^{-5}. These values clearly indicates that the contribution of ”anisotropic” dipolar relaxation mechanisms to ^{1}H STD signals can be neglected, and hence the ^{1}H STD signals are not biased by molecule orientation in PBLG-based lyotropic systems.

Qualitative STD-NMR study on three model chiral alcohols. In this exploratory work, anisotropic ^{1}H STD-NMR experiments are carried out on three chiral secondary alcohols (**PL**, **BL** and **HL**), sharing a common hydroxyl, methyl and methine group on the stereogenic center, but three different fourth substituents (rigid or flexible moiety) (see **Figure 2a**). All of them are characterized by a marked molecular shape anisotropy around the stereogenic center (see **Figure 2b**), while **PL** and **BL** have been abundantly exploited as model analytes to evaluate the enantiodiscriminating capability of various chiral mesophases by ^{13}C, ^{2}H or NAD NMR.[26,40,41,42] With respect to molecular interactions, the donor proton of the OH group can *a priori* easily

establish an H-bonding (-OH) with the carbonyl site of the PBLG side-chains, while the aromatic and acetylenic substituents can provide π-π interactions (or even π-stacking) with the terminal aromatic ring of the polymer.[43,44,45]

To qualitatively evaluate their respective interactions with the polymer side-chain, STD-NMR experiments are performed using identical experimental conditions for the sample preparation. Thus, the polarity of the co-solvent (CD_2Cl_2), ratios of PBLG/co-solvent ($w_{PBLG}/w_{co\text{-}solv.}$) or PBLG/total weight ($w_{PBLG}/w_{Tot.}$) as well as molar quantity in analyte have been kept constant (see **Table SI-1**). Each enantiomer of the three chiral analytes (**HL**, **PL**, **BL**) are analyzed separately, with the exception of **HL** for which only samples of (*S*)-**HL** and (*S/R*)-**HL** have been considered. Anisotropic ^{1}H STD spectra and the subsequent site-specific STD amplification factors, $STD_i^{R,S}(\%)$, are given for each of them in the SI with data listed in **Tables SI-2** to **S-4**). A visual chart of hydrogen sites giving rise to signals on the anisotropic STD-NMR spectra are highlighted in **Figure 2c**.

Anisotropic ^{1}H STD spectra of these three chiral alcohols show a significant STD signal for the hydroxyl group (OH), thus pointing out the common occurrence of H-bonding with the carbonyl group of PBLG, as initially anticipated. The STD amplification factors for other sites are really contrasted according to the nature of the substituents attached to the stereogenic center (see **Figure 2a**). In particular, no STD signals are detected on the spectrum of **HL** except for the OH group (see **Figure 2c**), showing a poor affinity of this saturated alcohol with PBLG (see **Figure SI-1**). In the case of the aromatic alcohol, **PL**, only relatively small STD signals arise from the hydrogen sites bonded to the stereogenic center or very closed (methine and methyl groups, respectively), while no STD signals is detected from the phenyl group, even increasing the number of scans.

Interestingly, these further STD signals (only observed at long saturation times (t_{sat} > 5 s)) are not associated to the same site in each enantiomer (the methine site for the (*S*)-isomer and methyl site for the (*R*)-isomer) (see **Figure 2c**). These differences in STD spectra clearly evidence a difference of enantiomeric orientation with respect to the external field B_0 in their “bound” state, namely when they strongly interact with the polymer side-chains.

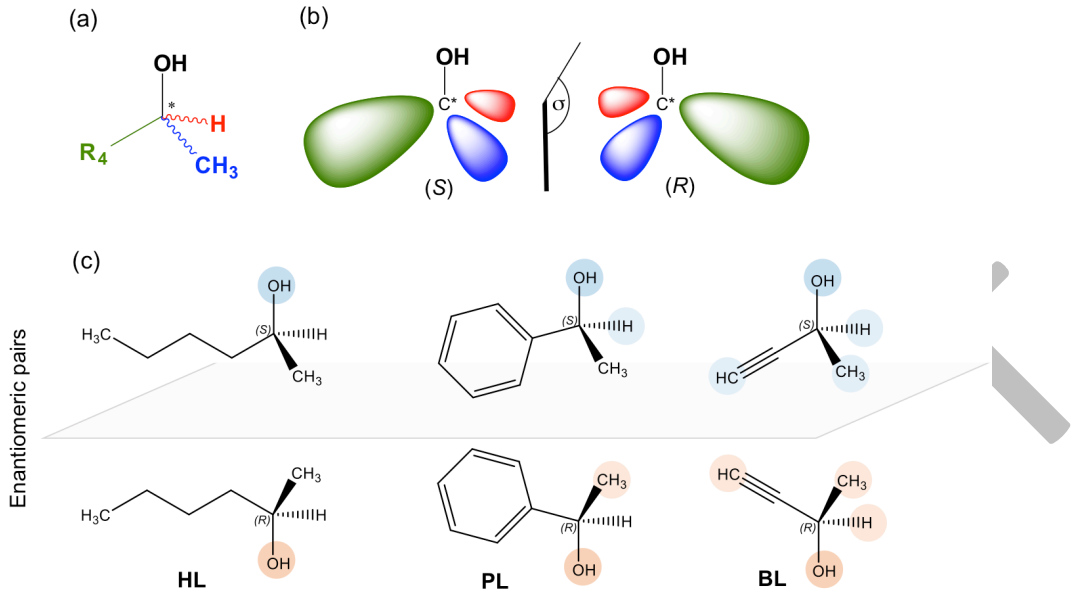

Figure 2. (a) Generic structure of model chiral molecules studied here where the R_4 substituent is a butyl, phenyl and ethynyl group. The color code used for each substituent (-OH (black), -H (red), $-CH_3$ (blue), $-R_4$ (green)) is applied throughout the article and in SI. (b) Crude schematic representation of the molecular shapes of four substituents around the stereogenic center. (c) Colorized view of hydrogen sites showing a significant ^{1}H STD effects in enantiomers of **HL**, **PL** and **BL,** depending on the intensity of their associated STD signal.

The highest STD amplification factors (%) are observed in the case of the acetylenic alcohol **BL** (see **Table SI-3**). For both enantiomers, all ^{1}H sites (see **Figure 2c)** exhibit a significant amplification factor on the ^{1}H STD spectrum (from 5.1 to 16.7%), including for the ethynyl group (see **Figure 3** and **Table SI-5**). These results clearly suggest an adequate/optimal spatial organization of the ethynyl moiety (and the whole molecule) towards the terminal aromatic group of the glutamic chain. This example appears to be the first direct proof of possible π-π interactions between unsaturated bounds of the solute and the aromatic ring of PBLG, and their important role in the enantiodiscrimination mechanism. The lack of noticeable STD effect visible on the aromatic ring of **PL,** for which π-π interactions could also be expected, could simply be understood as a consequence of higher steric hindrance around the asymmetric carbon that prevents an easy interaction with the glutamic phenyl group (in the inner space between to side-chains) (see **Figure SI-1**).

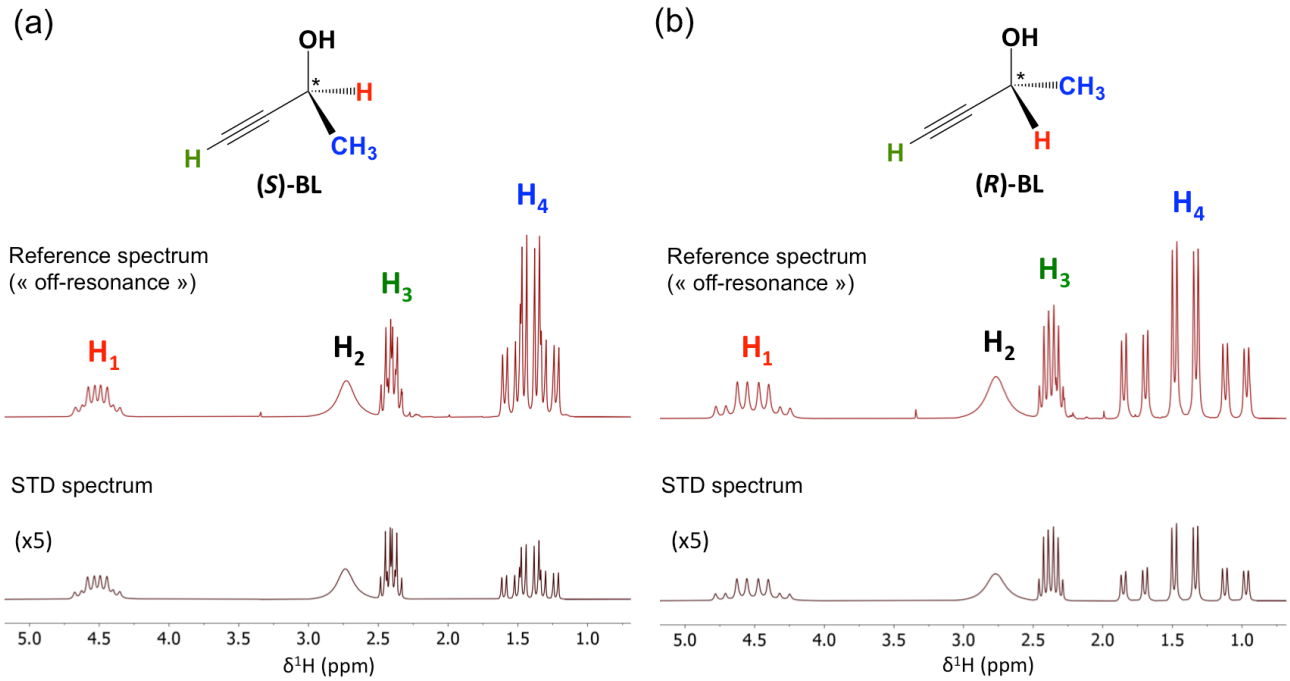

Figure 3. (a) Reference anisotropic 600 MHz ^{1}H NMR spectra of the (*S*)-**BL** (a) and (*R*)-**BL** dissolved in PBLG/CD_2Cl_2 (275 K), respectively. (b) ^{1}H STD-NMR spectrum of **BL** obtained after subtraction of spectra recorded with/without saturation of PBLG. The ^{1}H STD experiments were carried out here with a t_{sat} of 6 s. Baseline correction was applied on both reference and STD spectra to remove the PBLG signal contribution. The ^{1}H STD spectra are displayed with a ×5 vertical zoom.

Finally, relative STD values from sites-to-sites vary from the (*S*)-isomer to the (*R*)-isomer of **BL**, suggesting once again that enantiomers are oriented differently at the vicinity of the polymer side-chains, and confirming the first observation with **PL**. This difference of epitope mapping between the two enantiomers towards PBLG during the binding process are further investigated in a quantitative manner in the following section.

Quantitative STD-NMR analysis of (R)- and (S)-BL in PBLG. Beyond the first qualitative study described above, a quantitative approach is then carried out to finely evaluate the variation of epitope mapping without possible experimental bias. We focus here on the case of **BL** as it delivers intense STD signals and well resolved spectral patterns for both isomers making it a suitable model for such an investigation. STD-NMR experiments are first performed on two separated samples of enantiopur *(S)*- and *(R)*-**BL** with the same composition, and prepared with the same protocol (see **Table SI-1**). The temperature is fixed at 275 K in order to circumvent the peak-overlap between the hydroxyl and the acetylenic signals.

As seen in **Figure 3a**, the comparison of anisotropic ^{1}H NMR spectra shows clear spectral enantiodiscriminations with large changes in the spectral patterns, especially for the methyl group. An even better spectral discrimination is obtained with other nuclei such as ^{13}C (see **Figures SI-14** and **SI-15**) or ^{2}H (see **Figure SI-16**). Each enantiomer shows significant STD signals with amplification factors higher than 5% for all the sites at a saturation time t_{sat} of 6 s, with however, variations of relative STD signals that may reflect different geometries of "enantiomer-polymer complex".

To assess this feature in a reliable way, a quantitative approach of STD-NMR in PBLG is considered. Indeed, in the first approach explored previously, there are several bias that may prevent a direct and reliable interpretation of STD signals in terms of internuclei distances and thus of relevant geometrical insights on the binding process. Possible biases are: i) a fast polymer-solute rebinding process during t_{sat},[28,46,47,48] and ii) a strong variation of longitudinal relaxation time, T_1(^{1}H), from site-to-site.[46,47,48] While the former is here negligible owing to the high solute-to-polymer ratio used in this work, the latter has to be considered, given the dispersion of T_1(^{1}H) at the atomic level (see **Section VII** in **SI**) and because t_{sat} is here higher than T_1(^{1}H) values. Although bias measurements arising from relaxation are, in principle, assumed to be identical for both enantiomers, small variations in viscosity due to imperfect reproducibility of the mesophase preparation cannot be excluded. To overcome such pitfalls, a build-up curve approach is performed where anisotropic STD-NMR experiments are repeated with an incrementing t_{sat} delay (see **Figure 4**). The amplification factor STD of a site *i* evolves as an asymptotic mono-exponential function of the saturation time, t_{sat}, according to **Eq. 4**.[46,47,48]

$$STD_i^{R,S}(t_{\mathrm{sat}}) = STD_{i,max}^{R,S}(t_{\mathrm{sat}})\left(1 - \mathrm{e}^{-k_{\mathrm{sat}}^{R,S} \times t_{\mathrm{sat}}}\right) \qquad (\mathbf{4})$$

where k_{sat} is the rate of saturation (equivalent to the slope of the curve) while the term $STD_{i,max}^{R,S}(t_{\mathrm{sat}})$ corresponds to the maximum amplification factor achieved by a given nuclei i (asymptote of the curve). After fitting the experimental values according to **Eq. 4**, it is possible to estimate the value of $STD_i^{R,S}$ for a t_{sat} tending towards zero, denoted $STD_0^{R,S}$, by calculating the product $STD_{max}^{R,S} \times k_{sat}^{R,S}$.[46,47] Thus, the $STD_0^{R,S}$ value is a quantity unbiased by the T_1 value of the site considered. This approach is a well-established procedure to extract quantitative data from STD 1D NMR experiments, and can be extended to anisotropic 1D NMR experiments.

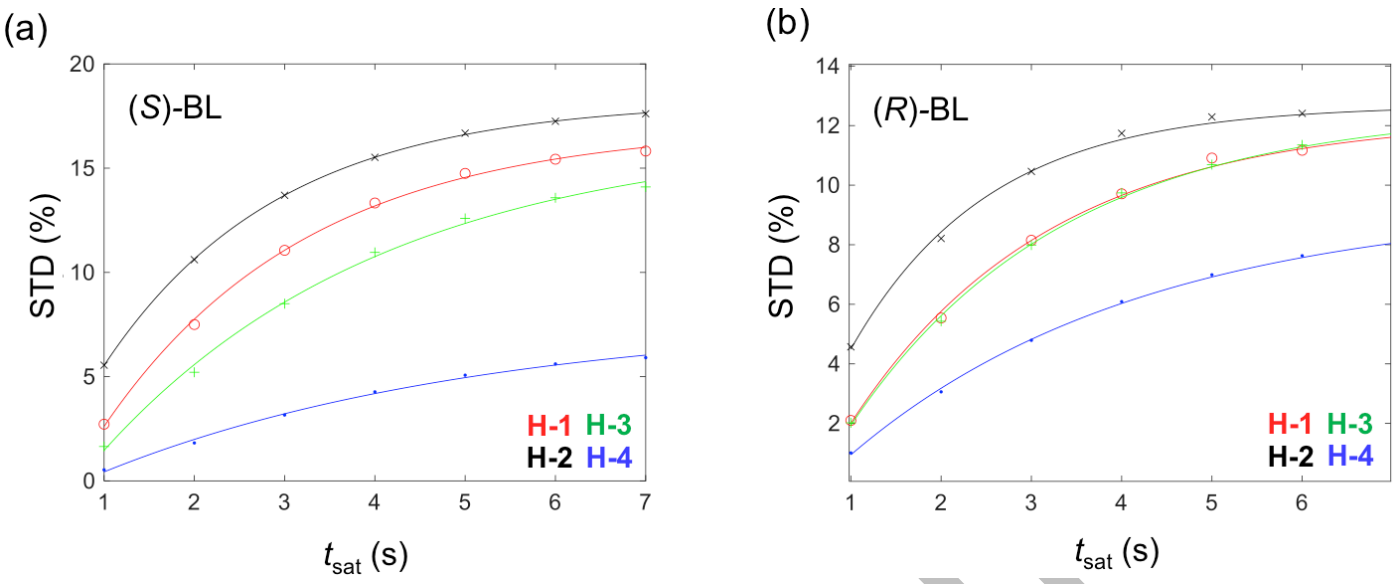

Figure 4. (a, b) Build-up curves providing STD % of (*S*)-**BL** and (*R*)-**BL** as a function of the saturation time (t_{sat}).

Table 1. Site-specific STD_0 (%) obtained for the two enantiopure oriented samples.

	(*S*)-BL				(*R*)-BL			
Sites	STD_{max}	k_{sat} (s^{-1})	STD_0 (%)	Relative STD_0 (%)	STD_{max}	k_{sat} (s^{-1})	STD_0 (%)	Relative STD_0 (%)
H-1	17.0 ± 0.8	0.44 ± 0.07	7.5 ± 1.2	80.0	12.3 ± 0.8	0.46 ± 0.10	5.6 ± 1.3	67.3
H-2	18.2 ± 0.1	0.52 ± 0.02	9.4 ± 0.3	100	12.7 ± 0.6	0.66 ± 0.16	8.4 ± 2.1	100
H-3	16.6 ± 2.0	0.32 ± 0.09	5.3 ± 1.7	56.0	12.6 ± 0.7	0.42 ± 0.07	5.3 ± 0.9	64.3
H-4	7.8 ± 1.6	0.24 ± 0.10	1.8 ± 0.9	19.7	9.4 ± 0.8	0.31 ± 0.06	2.9 ± 0.6	34.8

[a]STD_0 (%) values are calculated after confidence interval.

This build-up curve protocol is performed on the two enantiopure oriented samples and the very good agreement between the experimental data and the analytical expression of **Eq. 4** is visible on **Figure 4**. Details about the goodness of the fit are available in **Section VII.3** of the **SI**. The $STD_0^{R,S}$ values for each site of (*R*/*S*)-**BL** are then determined and listed in **Table 1**, along with the associated fitting parameters. All the values are given with a 95% confidence interval. The STD_0 values for both enantiomers are in the same order of magnitude, with comparable total STD_0 (24.0% and 22.1% for (*S*) and (*R*)-isomers, respectively) reflecting a similar affinity towards the chiral polymer. Another common feature is the maximal STD_0 reached for the hydroxyl group (H-2), showing that H-bonding plays a central role in the polymer-solute interaction. Yet, the variation of STD_0 values from site-to-site is quite different between the two enantiomers. This can be assessed

by calculating the relative STD_0 factors where the proton with the highest STD_0 amplification factor is arbitrarily fixed at 100% and the values from the other hydrogens are then determined relative to this site. As shown in **Table 1** and **Figure 5b**, the relative STD_0 values are significantly different from one enantiomer to the other, in particular regarding the methine and methyl sites. This variation of epitope mapping confirmed by a quantitative STD approach highlights different orientations of the two enantiomers during the binding process. In other words, the enantio-discrimination phenomenon is here mostly driven by diastereomorphous interactions between solutes in the bound state and the polymer -chains, *i.e.* $\langle S_{\alpha\beta}\rangle_b^R \neq \langle S_{\alpha\beta}\rangle_b^S$, rather than a difference in affinity with respect to PBLG.

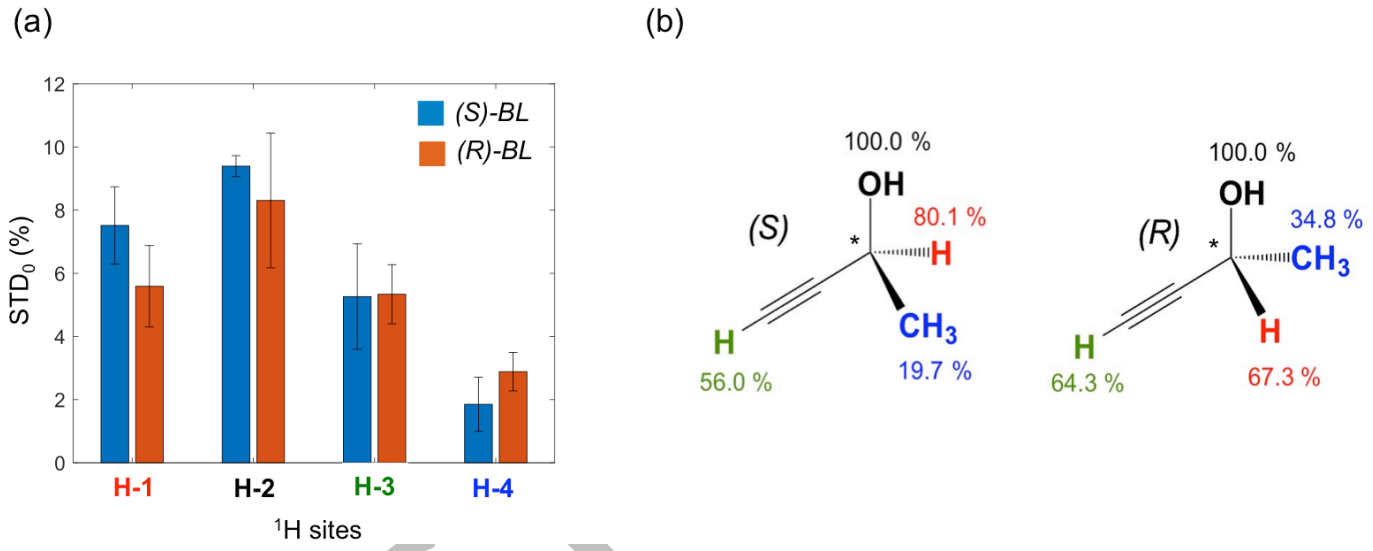

Figure 5. (a) Plot of variation of STD_0 (%) *versus* the molecular sites (H-1 to H-4.) for the (*R*)- and (*S*)-isomer of **BL** in PBLG, recorded separately. Error bars correspond to 95% confidence intervals. (b) Epitope mapping of the (*S*)- and (*R*)-**BL** binding the polymer side-chains for sites H-1 to H-4. Values correspond to the relative STD_0 % after build-up curve fitting.

STD-NMR analysis of (R/S)-BL in PBLG. While the STD-NMR data collected on separated samples have established differences of interactions between the enantiomers of **BL** with PBLG, we have investigated whether this difference still exists in racemic series. Indeed, a competitive binding process between both enantiomers may lead to different STD features than the ones observed in the enantiopure samples.

In this perspective, a STD experiment is performed on a racemic series of *(R/S)*-**BL** dissolved in PBLG/CD_2Cl_2 and the subsequent STD spectrum shows significant signals for each hydrogen site. To screen STD differences between the two enantiomers, it is necessary to assign signals to both. **BL** provides relevant spectral features for such a study as its enantiomers lead to

significantly different (^{1}H-^{1}H)-RDCs and ^{1}H-RCSAs, so that some signals can be assigned unambiguously on 1D ^{1}H spectrum (see **Figure 6**). This assignment of each line has been supported by comparison with the ^{1}H signals measured on the enantiopure samples. Note, however, that the hydroxyl groups (sites H-2) of the enantiomers resonate at the same frequency due to fast chemical exchange. Thus, this signal cannot be here exploited to track STD differences for the two enantiomers (see **Figure SI-10**).

Comparison of anisotropic STD-NMR and reference spectra of ***(R/S)*-BL** points out variations of ^{1}H STD signals for each enantiomer. This is clearly observed in the methyl region (H-4) on **Figure 6c** where lines assigned to (*S*)-**BL** are less intense compared to the ones from the (*R*)-isomer. A similar observation (but less significant) can be done for the alcynic proton H-3 (see **Figure 6b**), while the STD signals at the site H-1 are identical for the (*R*)- and (*S*)-enantiomers (see **Figure 6a**). As in the case of enantiopure samples, these results highlight enantioselective interactions during the binding process with the PBLG side-chains in a racemic mixture. The enantiospecific solute-polymer complex shows geometrical differences reminiscent of those observed previously, but with some differences.

In one hand, both enantiomers in the bound state are oriented so that the methyl group is the farthest site from the polymer, and once again, this feature is more pronounced for the (*S*)-isomer. In another hand, the identical STD signals for both enantiomers at the site H-1 suggest methine at a same distance from PBLG, which is not the case in enantiopure sample where different STD_0 values have been determined (7.5 *vs.* 5.6 %) as seen in **Table 1**. Therefore, the presence of both enantiomers dissolved in a same chiral mesophase still leads to enantioselective interactions with respect to PBLG, but with slight changes in the orientation of enantiomers at the vicinity of the polymer.

Unsurprisingly, this affects the magnitude of RDC(^{1}H-^{1}H)s in both oriented samples. The absolute values of the total couplings constants, T(^{1}H-^{1}H) = J(^{1}H-^{1}H)+ 2D(^{1}H-^{1}H), within the methyl pattern (A_3MX spin system) range from $\left|T^R_{\mathrm{A}_3}(ee = 100\%)\right|$ = 219 Hz, $|T^R_{\mathrm{AM}}(ee = 100\%)|$ = 92.9 Hz and $|T^R_{\mathrm{AX}}(ee = 100\%)|$ = 19.7 Hz to $\left|T^R_{\mathrm{A}_3}(ee = 0\%)\right|$ = 172.8 Hz, $|T^R_{\mathrm{AM}}(ee = 0\%)|$ = 76.8 Hz and $|T^R_{\mathrm{AX}}(ee = 0\%)|$ = 15.0 Hz for the (*R*)-isomer, and from $\left|T^S_{\mathrm{A}_3}(ee = 100\%)\right| = 83.4$ Hz, $\left|T^S_{\mathrm{AM}}(ee = 100\%)\right| = 54.9$ Hz and $\left|T^S_{\mathrm{AX}}(ee = 100\%)\right| = 20.5$ Hz to ($\left|T^S_{\mathrm{A}_3}(ee = 0\%)\right|$ = 64.9 Hz, $\left|T^S_{\mathrm{AM}}(ee = 0\%)\right|$ = 50.2 Hz, $\left|T^S_{\mathrm{AX}}(ee = 0\%)\right|$ = 15.9 Hz for the (*S*)-isomer. Thus, the (*R*)- and (*S*)-isomers show a decrease of

about 20% in average in all three coupling constants, with a variation dropping to 10% for the second coupling constant T_{AM} for the (*S*)-isomer.

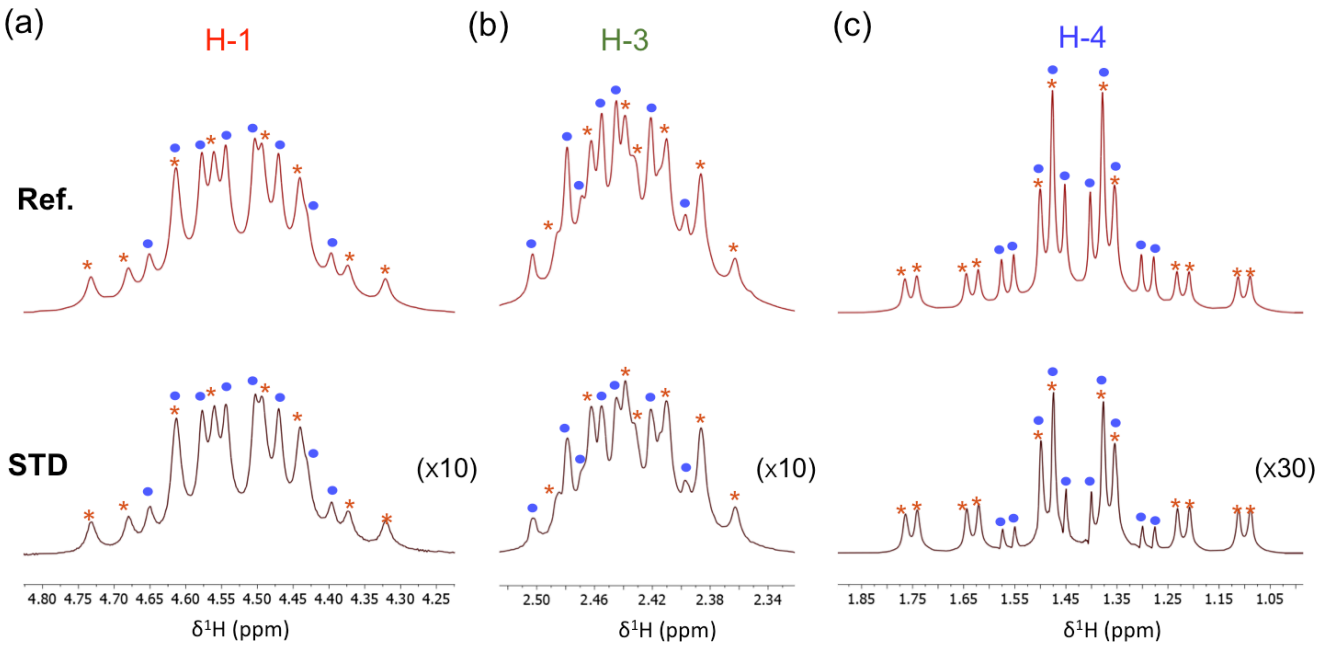

Figure 6. Comparison between anisotropic reference (top row) and STD spectra (bottom row) recorded on a racemic sample of (*R/S*)-**BL** dissolved in a PBLG/CD_2Cl_2 mesophase. The STD experiment is performed in 32 scans with a t_{sat} of 6 s. Zooms on the (a) methyl, (b) methine and (c) ethynyl group regions are given. To ease the comparison, STD spectra are displayed at different scales as specified in brackets. Lines from (*S*)- and (*R*)-isomers are tagged by blue solid circles and orange stars, respectively. The assignment shown is obtained by comparison with the signals observed on the enantiopure samples.

STD-NMR analysis of (R/S)-BL in the achiral PBG phase. First STD results collected with an enantiopure or racemic mixture of **BL** clearly reveal again interactions with the polypeptide chain with a noticeable difference of epitope mapping between the complex (*R*)-**BL**/PBLG and (*S*)-**BL**/PBLG. Combined with the molecular shape anisotropy of **BL**, these differences of intermolecular interactions in the "bound" complex participate to the enantiodiscrimination mechanisms involving the chirality of the solute and polymer.

An interesting situation exists when the enantiomers of (*R/S*)-**BL** are dissolved in a mesophase made of a racemic mixture of PBLG and PBDG, its enantiomers (right and left handness helix). In the fast exchange regime for the solute, this orienting system becomes achiral by compensation, preventing all enantiodiscrimination phenomena to be observed in average.[49] Under these conditions, one might expect similar STD spectra for both enantiomers in such an achiral medium.

To answer to this intriguing question, ^{1}H STD-NMR experiments are carried on (*R/S*)-**BL** oriented in the PBG achiral mesophase (PBG/CD_2Cl_2) (see **Table SI-1**). Only the hydroxyl groups give rise to a STD signal, unlike to the other hydrogen sites. This result is very different from those obtained with a chiral mesophase. What that suggests remains a matter of hypothesis at this level. One potential explanation relies on the three-sites exchanging system whereby each enantiomer (*R* or *S*) is in fast exchange with the *L*- and *D*-polymer. From this dynamic point of view, the time-residences of the different enantiomer-polymer arrays might significantly decrease, preventing any efficient intermolecular magnetization transfer between solutes and polymer, and hence the absence of detectable STD signals.

Experimental section

NMR sample. Samples are approximately prepared with ~15 mg of enantiomer each, ~100 mg of PBLG (DP = 800) and ~600 mg of dry CD_2Cl_2 with m_{PBLG}/m_{tot} of ~14 %. Details for the sample compositions and their preparation (fire-sealed tubes) are reported in the **Supp. Info** (see **Table SI-1**).

NMR experiments. All anisotropic ^{1}H NMR and ^{1}H STD-NMR spectra were recorded on a 14.1 T Bruker (Avance II) NMR spectrometer equipped by a 5-mm ^{2}H selective cryogenic probe operating at 600.13 MHz for ^{1}H. Specific experimental details are given in the figure captions or in the **SI**. If not otherwise specified, the sample temperature was set to 295 K.

From practical point of view, the routine ^{1}H STD pulse sequence could be applied with no peculiar modification (see **Figure SI-2**). In the “on-experiment”, polymer spins were saturated by a train of 50 ms Gaussian selective pulses - applied during the preparation step - with a total time corresponding to the saturation time t_{sat}. The selective pulse frequency offset was fixed to selectively saturate the polymer nuclei while leaving solutes undisturbed. The choice of this frequency offset was optimized to yield maximal STD amplification factors (see **Figure SI-3**). The off-experiment was carried out in exact similar conditions but in the absence of saturation. In order to limit the impact of instrumental instabilities of the spectrometer, the acquisition of "on/off-resonance" spectra can be alternated.

To deal with the ^{1}H NMR contribution from polymer, integration was performed after a tailored baseline correction, *i.e.* Whittaker Smother algorithm (provided by MestreNova). This procedure enabled more repeatable integration values than the one obtained after a CPMG (Carr-Purcell-

Meiboom-Gill) filter.[50] The latter option suffered from phase distortions due to the difficulty of cancelling the total spin-spin coupling modulation (T_{HH}) even for short echo times.

Conclusion

Establishing and then prioritizing the key molecular features governing the molecular shape recognition mechanisms involved in enantiodiscrimination phenomena in lyotropic CLCs is essential for two reasons:[51,52,53] i) optimize computational predictions (such as molecular dynamics simulation) of existing enantiodiscriminating helically-chiral polymers with ultimate goal of solving the thorny challenge of absolute configuration determination, ii) design novel polymer-based effective enantiodiscriminating systems.

So far the majority of experimental studies dedicated to this purpose are based on the evaluation of molecular order parameters for each enantiomer (Saupe's matrix parameters) and the analysis of their orientational difference (through the comparison of alignment tensors: variation of principal axis direction, 9D angle, …). In this work, we propose a paradigm shift by directly characterizing the transient complex formed by the enantiomers and the orienting chiral polymer with the help of ^{1}H STD-NMR experiments.

Interestingly, we demonstrate that this approach allows to experimentally determine the active interaction sites between enantiomers and the PBLG side-chains and how enantiomers can spatially interact differently with them. Furthermore, this method supported by a build-up curve approach, enables a direct and unbiased comparison of the orientation of enantiomers at the vicinity of the polymer side-chains.

This first-ever experimental STD study offers great hope and paves the way to the screening of series of model molecules in order to evaluate their interactions with accessible fragments of polymer as PBLG, but also with other polypeptide chiral polymers (such as PELG or PCBLL[54,55] or new polymers more recently designed such as PSMBLG, PBPMLG, …),[56,57] as well as other enantiodiscriminating chiral polymer families such as polyacetylenes.[19,22,58]

Finally, to further study pairs of enantiomers dissolved in a single oriented sample, including STD scheme into bi-dimensional NMR experiments should be valuable in case of complex an overlapped ^{1}H STD spectra. An alternative strategy involving proton-decoupled ^{13}C-NMR detection of STD spectra could also be very effective, not least because the ^{13}C-{^{1}H} signals of enantiomers in the PBLG phases can be discriminated on the basis of differences of residual ^{13}C chemical shift

anisotropies (^{13}C-RCSA) (see ^{13}C-{^{1}H} 1D NMR spectra in **SI**).[1,2,40,59] New investigations exploring these two options are currently in progress.

Acknowledgments

P.L. and B.G. acknowledges the CNRS for its recurrent funding of fundamental research and the Université Paris-Saclay for its support, as well as Juliette Delay for her participation to this project in the frame of her first year of Master student's internship.

Conflict of Interest

The authors declare no conflict of interest.

Data Availability Statement

The data that support the findings of this study are available in ESI and from the corresponding author upon reasonable request.

References

[1] C. Aroulanda, P. Lesot, Chirality. ***2022***, 34, 182-244.

[2] P. Lesot, C. Aroulanda, P. Berdagué, A. Meddour, D. Merlet, J. Farjon, N. Giraud, O. Lafon, Prog. Nucl. Magn. Reson. Spectrosc. ***2020***, 116, 85-154.

[3] J. Shen, Y. Okamoto, Chem. Rev. ***2016***, 116, 1094-1138.

[4] P. Lesot, Y. Gounelle, D. Merlet, A. Loewenstein, J. Courtieu, J. Phys. Chem. A. ***1995***, 99, 14871-14875.

[5] J. Courtieu, C. Aroulanda, P. Lesot, A. Meddour, D. Merlet, Liq. Crystals. ***2010***, 37, 903-912.

[6] M. Sarfati, P. Lesot, D. Merlet and J. Courtieu, Chem. Commun. ***2000***, 2069-2081.

[7] F. Hallwass, M. Schmidt, H. Sun, A. Mazur, G. Kummerlöwe, B. Luy, A. Navarro-Vázquez, C. Griesinger, U. M. Reinscheid, Angew. Chem., Int. Ed. ***2011***, 50, 9487-9490.

[8] A. Navarro-Vazquez, R. Gil, K. Blinov, J. Nat. Prod. **2018**, 81, 203-210.

[9] Y. Liu, A. Navarro-Vázquez, R. R. Gil, C. Griesinger, G. E. Martin, R. T. Williamson, Nature Protocol ***2018***, 14, 217-247.

[10] P. Lesot, R. R. Gil, P. Berdagué, A. Navarro-Vazquez, J. Nat. Prod. ***2020***, 833, 141-3148.

[11] P. Berdagué, B. Gouilleux, M. Nolls, S. Immel, M. Reggelin, P. Lesot, Phys. Chem. Chem. Phys. ***2022***, 24, 7338-7348.

[12] P. Berdagué, E. Herbert-Puchetta, V. Jha, A. Panossian, F. Leroux, P. Lesot, New J. Chem. ***2015***, 39, 9504-9517.

[13] N. Nandi, J. Phys. Chem. B. ***2004***, 108, 789-797.

[14] J. Helfrich, J. Hentschk, U. M. Apel, Macromolecules ***1994***, 2, 472-482.

[15] Z. Serhan, I. Billault, A. Borgogno, A. Ferrarini, P. Lesot, Chem. Eur. J. ***2012***, 18, 117-126.

[16] A.O. Frank, J. C. Freudenberger, A. K. Shaytan, H. Kessler, B. Luy, Magn. Reson. Chem. **2015**, 53, 213-217.

[17] A. Ibanez de Opakua, F. Klama, I. E. Ndukwe, G. E. Martin, T. Williamson, M. Zweckstetter, Angew. Chem., Int. Ed. ***2020***, 59, 6172-6176.

[18] E. Sage, P. Tzvetkova, A. D. Gossert, P. Piechon, B. Luy, Chem. Eur. J. ***2020***, 26, 14435-14444.

[19] A. Krupp and M. Reggelin, Magn. Reson. Chem. ***2012***, 50, S45**-**S52.

[20] Schmidt, H. Sun, A. Leonov, C. Griesinger, U. M. Reinscheid, Magn. Reson. Chem. ***2012***, 50, S38**-**S44.

[21] Schwab, D. Herold, C.-M. Thiele, Chem. Eur. J. ***2017***, 23, 14576-14584.

[22] A. Krupp, M. Noll, M. Reggelin, Magn. Reson. Chem. ***2020***, 59, 577-586.

[23] A. Marx, B. Boettcher, C.-M. Thiele, Chem. Eur. J. ***2010***, 16, 1656-1660.

[24] A. Meddour, D. Atkinson, A. Loewenstein, J. Courtieu, Chem. Eur. J. ***1998***, 4, 1142-1147.

[25] J. W. Emsley and J. C. Lindon, in NMR Spectroscopy Using Liquid Crystal Solvents, Pergamon Press, Oxford, 1975.

[26] Lesot, D. Merlet, J. Courtieu, J.W. Emsley, T. T. Rantala, J. Jokisaari, J. Phys. Chem. A. ***1997***, 101, 5719-5724.

[27] M. Mayer, B. Meyer, Angew. Chem., Int. Ed. ***1999***, 38, 1784-1788.

[28] M. Gairí, M. Feliz, J. García, "Saturation transfer difference spectroscopy", in Encyclopedia of Analytical Chemistry, *2006*, 1-17, DOI: 10.1002/9780470027318.a9498. Print ISBN: 9780471976707| Online ISBN: 9780470027318.

[29] B. Meyer, T. Peters, Angew. Chem., Int. Ed. ***2003***. 42, 864-890.

[30] V. V. Krishnan, Cur. Anal. Chem. ***2005***, 1, 307-320.

[31] J. L. Wagstaff, S. L. Taylor, M. J. Howard, Mol. BioSyst. ***2013***, 9, 571-577.

[32] A. Shamshir, N. Phuoc Dinh, T. Jonsson, T. Sparrman, K. Irgum, J. of Chromatogr. A, ***2020***, 1623, 461130,1-12.

[33] B. A. Becker, C.K. Larive, J. Phys. Chem. B. ***2008***, 112, 13581-13587.

[34] D. M. Dias, J. M. C. Teixeira, I. Kuprov, E. J. New, D. Parker, Carlos F. G. C. Geraldes, Org. Biomol. Chem. ***2011***, 9, 5047-5050.

[35] C. Hamark, R. Pendrill, J. Landström, A. Dotson Fagerström, M. Sandgren, J. Stahlberg, G. Widmalm, Chem. Eur. J. ***2018***, 24, 17975-17985.

[36] S. Della Volpe, R. Listro, M. Parafioriti, M. Di Giacomo, D. Rossi, F. A. Ambrosio, G. Costa, ACS Med. Chem. Lett. ***2020***, 11, 883-888.

[37] V. Jayalakshmi, N. R. Krishna, J. Magn. Reson. ***2002***, 155, 106-118.

[38] T.C. Lubensky, Phys. Rev. A2, **1970**, 2497-2514.

[39] R.R. Vold, in: J.W. Emsley, (Ed.), Nuclear Magnetic Resonances of Liquid Crystals, NATO ASI Series, Dordrecht, 1985 pp. 253-288. (Chapter 11).

[40] A. Meddour, I. Canet, A. Loewenstein, J. M. Péchiné, J. Courtieu, J. Am. Chem. Soc. ***1994***, 116, 9652-9656.

[41] Meddour, P. Berdagué, A. Hedli, J. Courtieu, P. Lesot, J. Am. Chem. Soc., ***1997***, 119, 4502-4508.

[42] P. Lesot, D. Merlet, A. Loewenstein, J. Courtieu, Tetrahedron: Asymmetry. ***1998***, 9, 1871-1881.

[43] E. Arunan, G. R. Desiraju, R. A. Klein, J. Sadlej, S. Scheiner, I. Alkorta, D. C. Clary, R. H. Crabtree, J. Dannenberg, Definition of the hydrogen bond (IUPAC Recommendations 2011), Pure and Applied Chemistry, ***2011***, 83, 1637**-**1641.

[44] C. R. Martinez and B. L. Iverson, Chemical Science. ***2012***, 3, 2191-2201.

[45] M. Lewis, C. Bagwill, L. Hardebeck, S. Wireduaah, "Modern Computational Approaches to Understanding Interactions of Aromatics". Aromatic Interactions: Frontiers in Knowledge and Application. England: RSC (2016). In D.W., Johnson Hof F. (Eds.), pp. 1-17.

[46] P. M. Angulo, Enriquez-Navas, P. M. Nieto, Chem. Eur. J., ***2010***, 26, 7803-7812.

[47] P. M. Angulo, P. M. Nieto, Eur. Biophysics J. ***2011***, 40, 1357-1369.

[48] C. Guzzi, J. C. Munoz-Garcia, P. M. Enriquez-Navas, J. Rojo, J. Angulo,P. M. Nieto, Pure Appl. Chem. ***2013***, 85, 1771-1787.

[49] C. Canlet, D. Merlet, P. Lesot, A. Meddour, A. Loewenstein, J. Courtieu, Tetrahedron: Asymmetry. ***2000***, 11, 1911**-**1918.

[50] ~~[46]~~ S. Meiboom and D. Gill, Rev. Sci. Instrum. **1*958***, 29, 688-691.

[51] P. Berdagué, J.-E., Herbert-Pucheta, V. Jha, A. Panossian, F. Leroux, P. Lesot, New J. Chem. ***2015***, 39, 9504-9517.

[52] H. J. Krabbe, H. Heggemeier, B. Schrader, E. H. Korte, Angew. Chem., Int. Ed. ***1977***, 16, 791-792.

[53] G.-W. Li, X.-J. Wang, X. Lei, N. Liu, Z.-Q. Wu, Macromol. Rapid Commun. ***2022***, 43, 2100898 (1-12).

[54] C. Aroulanda, M. Sarfati, J. Courtieu, P. Lesot, Enantiomer ***2001***, 6, 281-287.

[55] S. Hansmann ,T. Larem, C.-M. Thiele, Eur. J. Org. Chem. ***2016***, 7, 1324-1329.

[56] S. Hansmann, V, Schmidts V, C.-M. Thiele, Chem. Eur. J. ***2017***, 23, 9114-9121.

[57] S. Jeziorowski, C.-M. Thiele, Chem. Eur. J. ***2018***, 24, 15631-15637.

[58] P. Lesot, P. Berdagué, A. Meddour, A. Kreiter, M. Noll, M. Reggelin, ChemPlusChem. ***2019***, 84, 144-153.

[59] C. Räuber, S. Berger, Magn. Reson. Chem., ***2010***, 48, 91-93.